Supporting information for

Chemical order or disorder -
A theoretical stability expose for expanding the
compositional space of quaternary metal borides

Martin Dahlqvist*, Johanna Rosen*

*Materials Design, Department of Physics, Chemistry and Biology (IFM), Linköping University,
SE-581 83 Linköping, Sweden*

* corresponding authors: martin.dahlqvist@liu.se; johanna.rosen@liu.se

This PDF file contains:

Schematic illustration of considered magnetic configurations for quaternary chemically ordered o-MAB phases (Figure S1)

Convergence test for plane-wave energy cut-off and k-point density (Figure S2).

Convergence test for size of supercells used to model chemical disorder, solid solution, for $(M'_{1-x}M''_x)_5AB_2$ MAB phases (Figure S3).

Calculated formation enthalpy as function of formation energy for M_5AB_2 phases (Figure S4).

Calculated formation enthalpy and identified equilibrium simplex for M_5AB_2 phases (Table S1).

Experimentally known ternary MAB phases (Table S2), quaternary solid solution MAB phases (Table S3) and quaternary chemically ordered o-MAB phases (Table S4).

Calculated thermodynamic stability of quaternary MAB phases evaluated at 0 K (Figure S5).

List of theoretically predicted stable o-MAB phases at 2000 K (Table S5).

List of theoretically predicted stable disorder solid solution MAB phases at 2000 K (Table S6).

Detailed structural information for o-MAB phases predicted stable (Table S7).

Atomic radius and electronegativity for considered M and A elements (Table S8).

Energy difference of o-MAB and disorder MAB compared with electronegativity of the metals (Figure S6).

Electronegativity difference as function of size difference for MAX phases (Figure S7).

Energy difference of o-MAB and disorder MAB compared with atomic size of the metals (Figure S8).

Calculated lattice parameters a and c colored based on the calculated stability (Figure S9).

Calculated lattice parameters a and c colored based on the size difference of the metals (Figure S10).
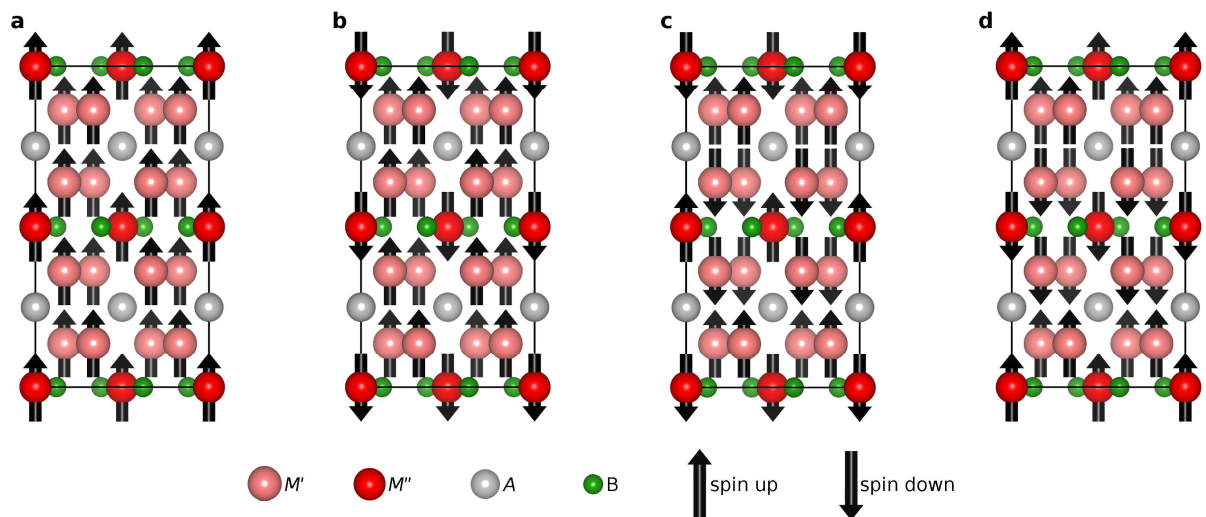
Figure S1. Schematic illustration of considered magnetic spin configurations for *o*-MAB phases. (a) FM, (b) AFM1, (c) AFM2, and (d) AFM3. These spin configurations were also modeled for structures with a disordered distribution of M' and M'' in a larger supercell (not shown here).
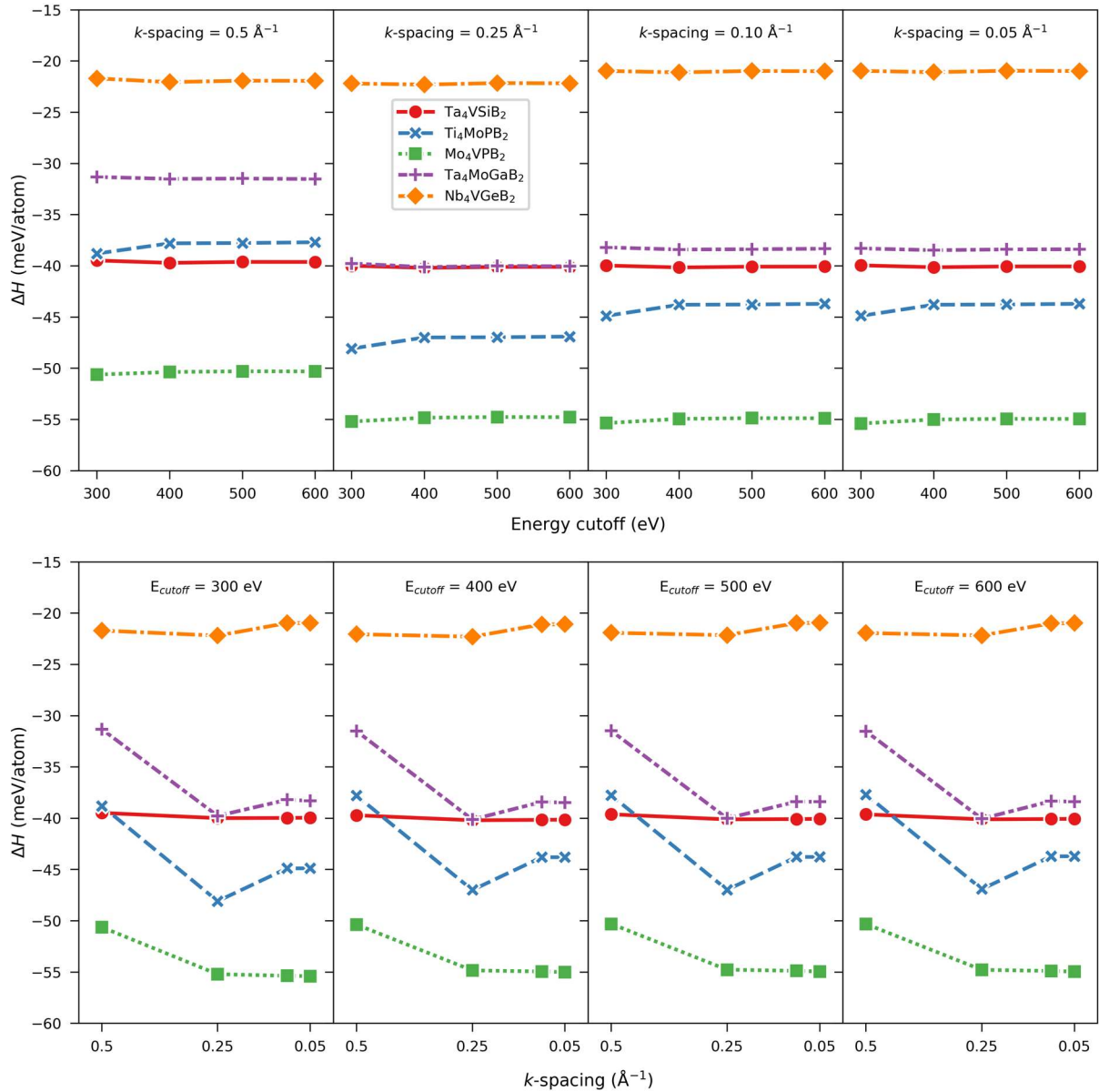
Figure S2. Demonstration for convergence of formation enthalpy ΔH_{cp} for five different o-MAB phases. Top panels show ΔH_{cp} as function of plane wave energy cutoff using four different k-point densities for the o-MAB phase and its competing phases. Bottom panels show ΔH_{cp} as function of k-point density for different plane wave energy cutoffs for the o-MAB phase and its competing phases. Using a plane wave energy cutoff pf 400 eV combined with a k-point density of 0.05 Å^{-1} ensures ΔH_{cp} values within less than 0.5 meV/atom as compared to using larger cutoff energies or denser k-point meshes.
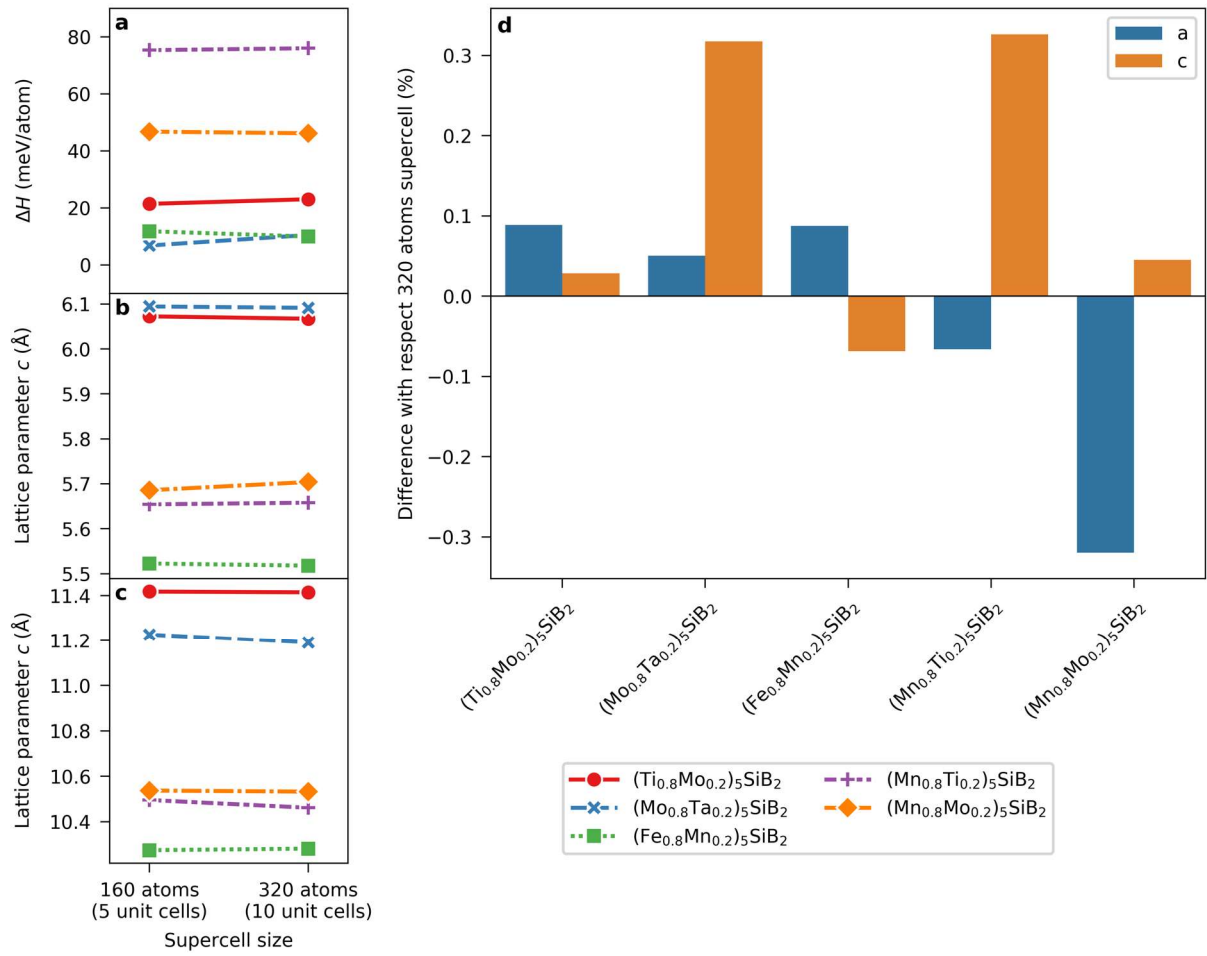
Figure S3. Size convergence of supercells used for modeling chemical disorder in $(M'_{0.8}M''_{0.2})_5 A B_2$. (a) Formation ΔH_{cp} enthalpy at 0 K, (b) lattice parameter a, (c) lattice parameter c as function of supercell size for five different compositions of $(M'_{0.8}M''_{0.2})_5 A B_2$. (d) Deviation of lattice parameters a and c for the smaller supercell size consisting of 160 atoms as compared to the larger supercell of 320 atoms.
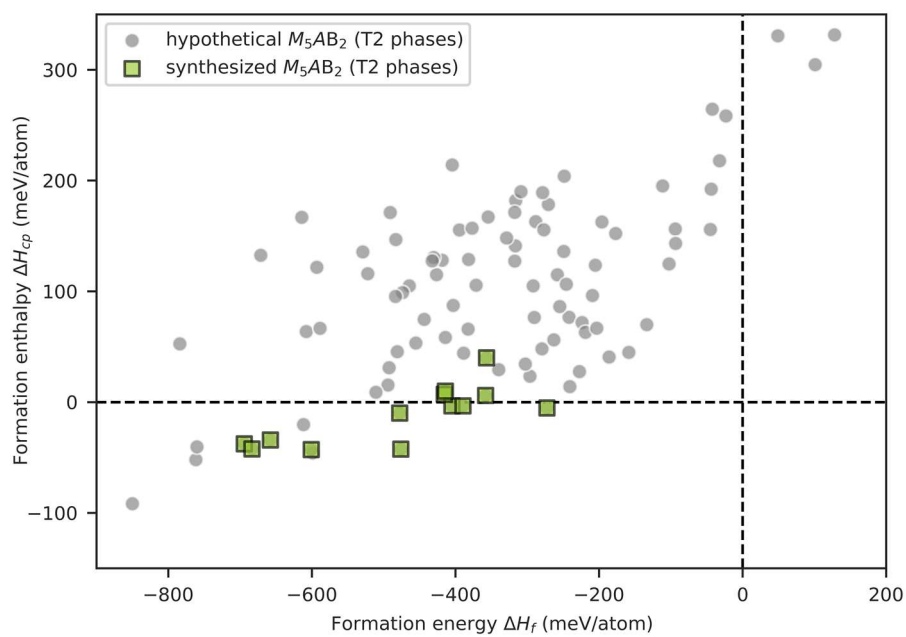
Figure S4. Calculated formation enthalpy as function of formation energy for M_5AB_2 phases. Experimentally reported M_5AB_2 phases are represented by green squares and hypothetical M_5AB_2 by grey circles.

Table S1. Calculated formation enthalpy ΔH_{cp} (in meV/atom) and identified equilibrium simplex for M_5AB_2 phases. Experimentally known M_5AB_2 phases are marked in bold.

M	A	ΔH_{cp} (meV/atom)	Equilibrium simplex	M	A	ΔH_{cp} (meV/atom)	Equilibrium simplex
Sc		127	Sc, ScB$_2$, Sc$_2$Al	Sc		95	Sc, ScB$_2$, Sc$_5$Ge$_3$
Y		152	Y, YB$_2$, Y$_2$Al	Y		171	Y, YB$_2$, Y$_5$Ge$_3$
Ti		155	TiB, Ti$_3$Al	Ti		67	TiB, Ti$_6$Ge$_2$B, Ti
Zr		167	Zr$_2$B, Zr$_3$Al, Zr	Zr		116	Zr, ZrB$_2$, Zr$_5$Ge$_3$
Hf		182	Hf, HfB$_2$, Hf$_4$Al$_3$	Hf		147	Hf, HfB$_2$, Hf$_2$Ge
V		75	V$_3$B$_2$, V$_3$Al, VAl$_3$	V		-20	VB, V$_3$Ge
Nb	Al	53	Nb$_3$B$_2$, Nb$_2$Al	Nb	Ge	-46	Nb$_3$B$_2$, Nb$_5$Ge$_3$, Nb
Ta		45	Ta$_3$B$_2$, Ta$_2$Al	**Ta**		**-43**	Ta$_3$B$_2$, Ta$_5$Ge$_3$, Ta$_3$Ge
Cr		124	Cr$_2$Al, Cr$_5$B$_3$, Cr$_2$AlB$_2$	Cr		56	CrB, Cr$_3$Ge
Mo		76	MoB, Mo$_3$Al	Mo		23	MoB, Mo$_3$Ge
W		41	W$_2$B, W, WAl$_5$	W		70	W$_2$B, W, Ge
Mn		115	Mn$_2$B, MnAl	Mn		34	Mn$_2$B, MnGe
Fe		77	Fe$_2$B, FeAl	Fe		14	Fe$_2$B, FeGe
Co		106	CoB, Co, CoAl	Co		28	Co$_2$B, CoGe
Sc		105	Sc, ScB$_2$, Sc$_5$Si$_3$	Sc		141	ScB$_2$, Sc$_3$In, Sc
Y		163	Y, YB$_2$, Y$_5$Si$_3$	Y		163	Y, YB$_2$, Y$_2$In
Ti		64	TiB, Ti$_6$Si$_2$B, Ti	Ti		148	TiB, Ti$_3$In
Zr		135	Zr, Zr$_2$Si, ZrB$_2$	Zr		190	ZrB$_2$, Zr$_3$In, Zr
Hf		171	Hf, HfB$_2$, Hf$_2$Si	Hf		178	Hf, Hf$_2$InB$_2$
V		**-38**	V$_3$B$_2$, V$_5$Si$_3$, V$_3$Si	V		204	V, In, V$_3$B$_2$
Nb	Si	**-34**	Nb$_3$B$_2$, Nb$_5$Si$_3$, Nb	Nb	In	105	Nb, In, Nb$_3$B$_2$
Ta		**-42**	Ta$_2$Si, Ta$_3$B$_2$	Ta		156	Ta, In, Ta$_3$B$_2$
Cr		44	CrB, Cr$_3$Si	Cr		331	Cr$_2$B, Cr, In
Mo		**-3**	MoB, Mo$_3$Si	Mo		218	Mo, MoB, In
W		**-5**	W$_2$B, WSi$_2$, W	W		331	W$_2$B, W, In
Mn		**7**	Mn$_2$B, MnSi	Mn		264	Mn$_2$B, Mn, In
Fe		**6**	Fe$_2$B, FeSi	Fe		192	Fe$_2$B, Fe, In
Co		29	CoB, Co$_2$Si, Co	Co		156	Co, CoB, In
Sc		122	Sc, ScB$_2$, Sc$_3$P$_2$	Sc		115	Sc, ScB$_2$, Sc$_5$Sn$_3$
Y		214	Y, YB$_2$, YP	Y		189	Y, YB$_2$, Y$_5$Sn$_3$
Ti		53	TiB, Ti$_3$P	Ti		130	TiB, Ti$_3$Sn
Zr		133	Zr, ZrB$_2$, Zr$_3$P	Zr		128	Zr, ZrB$_2$, Zr$_5$Sn$_3$
Hf		167	Hf, HfB$_2$, Hf$_3$P	Hf		129	Hf, HfB$_2$, Hf$_5$Sn$_3$
V		-92	VB, V$_3$P	V		106	V$_3$B$_2$, V$_3$Sn, VSn$_2$
Nb	P	-52	NbB, Nb$_3$P	Nb	Sn	58	NbB, Nb$_3$Sn
Ta		-40	TaB, Ta$_3$P	Ta		66	Ta$_3$B$_2$, Ta$_3$Sn, Sn
Cr		**-42**	CrB, Cr$_3$P	Cr		258	Cr$_2$B, Cr, Sn
Mo		**10**	MoB, Mo$_3$P	Mo		156	Mo, MoB, Sn
W		72	W$_2$B, WP	W		305	W$_2$B, W, Sn
Mn		**-10**	Mn$_2$B, MnB, Mn$_2$P	Mn		195	Mn$_2$B, Mn, Sn
Fe		**-3**	Fe$_2$B, FeP	Fe		143	Fe$_2$B, FeSn
Co		**40**	CoB, Co$_2$P, Co	Co		125	CoB, Co, CoSn
Sc		87	Sc, ScB$_2$, Sc$_5$Ga$_3$				
Y		136	Y, YB$_2$, Y$_5$Ga$_3$				
Ti		99	TiB, Ti$_3$Ga				
Zr		128	Zr, Zr$_2$Ga, ZrB$_2$				
Hf		157	Hf, Hf$_2$Ga, HfB$_2$				
V		31	V$_3$B$_2$, V$_3$Ga, V$_6$Ga$_5$				
Nb		15	Nb$_3$B$_2$, Nb$_5$Ga$_3$, Nb				
Ta	Ga	9	Ta, Ta$_3$B$_2$, Ta$_5$Ga$_3$B				
Cr		96	Cr$_2$B, Cr, CrGa$_4$				
Mo		48	MoB, Mo$_3$Ga				
W		45	W$_2$B, W, Ga				
Mn		86	Mn$_2$B, Mn$_3$Ga, MnGa$_4$				
Fe		63	Fe$_2$B, FeGa$_3$, Fe$_3$Ga				
Co		67	Co, CoB, CoGa				

Table S2. Experimentally reported ternary T2 phases.

Phase	References
V_5SiB_2†	1
Nb_5SiB_2	2, 3
Ta_5SiB_2	4-6
Mo_5SiB_2	7, 8
W_5SiB_2	7, 9
Mn_5SiB_2	10
Fe_5SiB_2	11-15
Co_5SiB_2‡	15
Ta_5GeB_2	16
Cr_5PB_2	17
Mo_5PB_2	18, 19
Mn_5PB_2	20
Fe_5PB_2	12, 14, 20, 21
Co_5PB_2	20

† Reported with 50 at% B at Si-site.
‡ Si partially occupy B-site with a Co_5Si_2B composition.

Table S3. Experimentally reported quaternary solid solution T2 phases with *M*-site chemical disorder.

Phase	References
$(Fe_{0.8}Mn_{0.2})_5SiB_2$	12
$(Fe_{0.8}Co_{0.2})_5SiB_2$	12, 15
$(Fe_{0.8}Mn_{0.2})_5PB_2$	12
$(Fe_{0.8}Co_{0.2})_5PB_2$	12, 21
$(Co_{0.7}Fe_{0.3})_5PB_2$	21
$(W_{0.96}Ta_{0.04})_5SiB_2$	22

Table S4. Experimentally reported quaternary T2 phases with *M*-site chemical order (*o*-MAB)

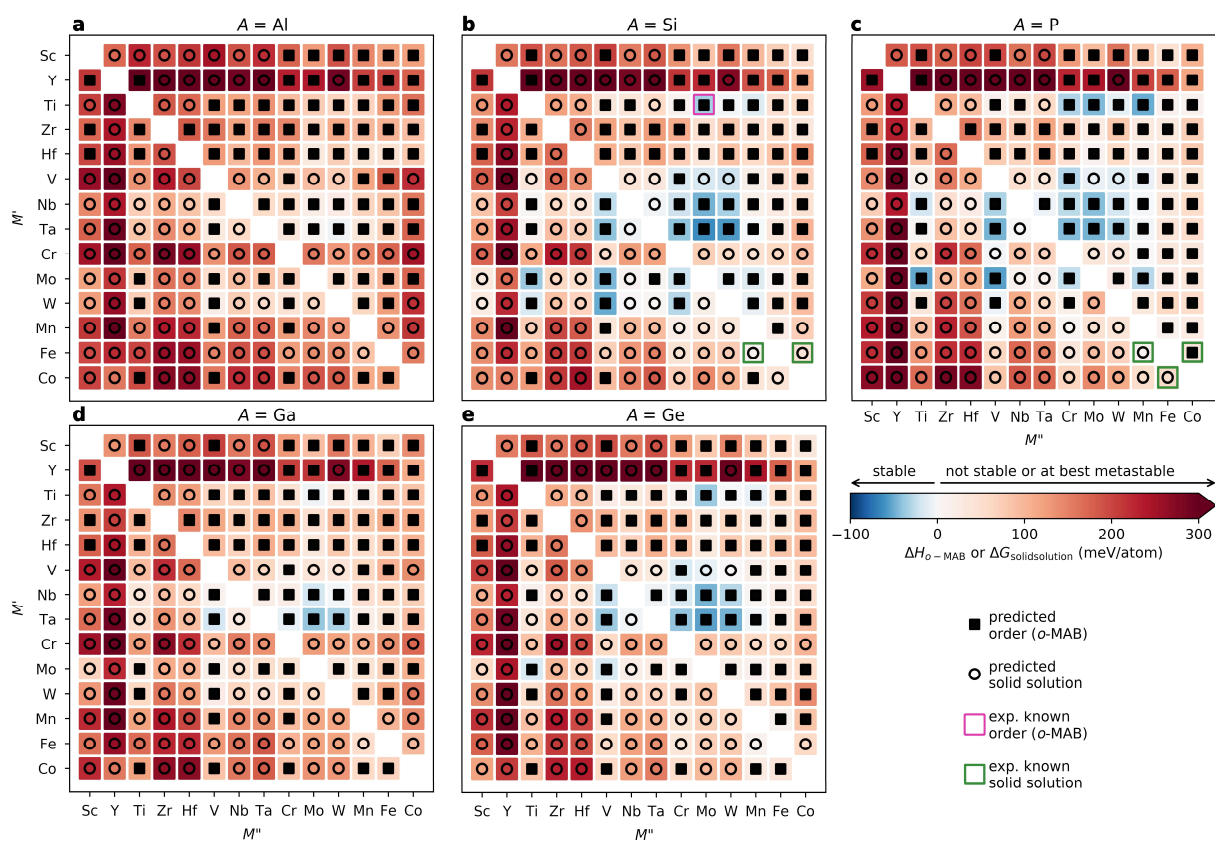| Year	Phase	References
2020	Ti_4MoSiB_2	23

Figure S5. Calculated formation enthalpy ΔH at 0 K for A = Al, Si, P, Ga, and Ge. Symbols represent chemical order of lowest energy at given M' and M'' with full square for ordered $M'_4 M'' A B_2$ o-MAB and open circle for solid solution $(M'_{0.8} M''_{0.2})_5 A B_2$.

Table S5. List of stable o-MAB phases, $M'_4M''A\mathrm{B}_2$, with their calculated formation enthalpy and identified equilibrium simplex. For comparison, the Gibbs free energy of formation is given for a disordered distribution of M' and M'', estimated at a typical synthesis temperature of 2000 K. These o-MAB phases fulfill the stability criteria $\Delta H_{o\text{-MAB}} < 0$ and $\Delta H_{o\text{-MAB}} - \Delta G_{\text{solid solution}} < 0$.

A	M'	M''	$\Delta H_{o\text{-MAB}}$ (meV/atom)	$\Delta G_{\text{solid solution}}$ (meV/atom)	Equilibrium simplex	Exp. reference
Si	Ti	Mo	-33	-31	TiB, Mo, $\mathrm{Ti_5Si_3}$, $\mathrm{Ti_6Si_2B}$	[23]
Si	Ti	Mn	-13	49	TiB, $\mathrm{TiMn_2}$, $\mathrm{Ti_5Si_3}$, $\mathrm{Ti_3B_4}$	
Si	Nb	V	-25	-20	$\mathrm{Nb_5SiB_2}$, $\mathrm{V_5SiB_2}$	
Si	Nb	Cr	-21	15	NbB, Cr, $\mathrm{Nb_5Si_3}$, $\mathrm{Nb_3B_2}$	
Si	Ta	V	-40	-29	$\mathrm{Ta_5SiB_2}$, $\mathrm{V_5SiB_2}$	
Si	Ta	Cr	-40	8	TaB, $\mathrm{Ta_5SiB_2}$, $\mathrm{Cr_3Si}$	
Si	Ta	Mn	-1	45	TaB, TaMnSi, $\mathrm{Ta_5SiB_2}$, $\mathrm{TaMn_2}$	
Si	Mo	V	-46	-41	VB, $\mathrm{Mo_5SiB_2}$, $\mathrm{Mo_3Si}$	
Si	Mo	Cr	-22	-11	$\mathrm{Mo_2CrB_2}$, $\mathrm{Mo_5Si_3}$, $\mathrm{Mo_3Si}$	
Si	Mo	Mn	-13	-6	$\mathrm{Mo_2MnB_2}$, $\mathrm{Mo_5Si_3}$, $\mathrm{Mo_3Si}$	
Si	W	Cr	-28	-25	$\mathrm{W_5SiB_2}$, CrB, $\mathrm{Cr_3Si}$	
P	Ti	Cr	-30	11	$\mathrm{TiB_2}$, $\mathrm{Ti_2P}$, $\mathrm{Ti_3P}$, $\mathrm{TiCr_2}$	
P	Ti	Mo	-44	-41	$\mathrm{TiB_2}$, $\mathrm{Ti_3P}$, Mo	
P	Ti	Mn	-49	31	$\mathrm{TiB_2}$, $\mathrm{Ti_3P}$, $\mathrm{Ti_2P}$, $\mathrm{TiMn_2}$	
P	Nb	V	-32	-14	$\mathrm{Nb_5PB_2}$, $\mathrm{V_5PB_2}$	
P	Nb	Cr	-27	19	$\mathrm{Nb_5PB_2}$, NbCrP, $\mathrm{Cr_2B}$, NbB	
P	Nb	Mn	-2	52	NbB, NbMnP, $\mathrm{Nb_5PB_2}$, $\mathrm{NbMn_2}$	
P	Ta	V	-46	-24	$\mathrm{Ta_5PB_2}$, $\mathrm{V_5PB_2}$	
P	Ta	Cr	-43	15	TaB, TaCrP, $\mathrm{Ta_5PB_2}$, Cr	
P	Ta	W	-32	-27	TaB, $\mathrm{Ta_2P}$, W	
P	Ta	Mn	-3	61	TaB, TaMnP, $\mathrm{Ta_5PB_2}$, $\mathrm{TaMn_2}$	
P	Mo	V	-55	-52	MoB, $\mathrm{Mo_3P}$, VB	
P	Mo	Cr	-25	-11	$\mathrm{Mo_2CrB_2}$, $\mathrm{Mo_3P}$, MoP	
P	Mo	Mn	-28	-1	$\mathrm{Mo_2MnB_2}$, MoP, $\mathrm{Mo_3P}$	
Ga	Ti	Mo	-4	14	TiB, $\mathrm{Ti_2Ga}$, Mo	
Ga	Ta	V	-17	-12	TaB, $\mathrm{Ta_5Ga_3}$, $\mathrm{V_3B_2}$, Ta	
Ga	Ta	Cr	-8	39	TaB, $\mathrm{TaCr_2}$, $\mathrm{Ta_5Ga_3}$, $\mathrm{CrGa_4}$	
Ga	Ta	W	-31	-28	TaB, W, $\mathrm{Ta_3B_2}$, $\mathrm{Ta_5Ga_3}$	
Ge	Ti	Mo	-37	-19	TiB, Mo, Ti, $\mathrm{Ti_5Ge_3}$	
Ge	Ti	W	-1	10	TiB, W, Ti, $\mathrm{Ti_5Ge_3}$	
Ge	Ti	Mn	-8	67	TiB, $\mathrm{TiMn_2}$, $\mathrm{Ti_5Ge_3}$, $\mathrm{Ti_3B_4}$	
Ge	Nb	V	-22	-21	$\mathrm{Nb_5GeB_2}$, $\mathrm{V_5B_6}$, $\mathrm{Nb_5Ge_3}$, $\mathrm{V_3Ge}$	
Ge	Nb	Cr	-16	14	NbB, Cr, $\mathrm{Nb_5Ge_3}$, $\mathrm{Nb_5GeB_2}$	
Ge	Ta	V	-36	-30	$\mathrm{Ta_5GeB_2}$, $\mathrm{V_5GeB_2}$	
Ge	Ta	Cr	-39	3	TaB, $\mathrm{Ta_5GeB_2}$, $\mathrm{Mo_3Ge}$	
Ge	Ta	Mn	-3	35	TaB, TaMnGe, $\mathrm{Ta_5GeB_2}$, $\mathrm{TaMn_2}$	

Table S6. List of stable solid solution phases, $(M'_{0.8}M''_{0.2})_5AB_2$, with Gibbs free energy of formation estimated at a typical synthesis temperature of 2000 K (given for a disordered distribution of M' and M'') and identified equilibrium simplex. For comparison, the calculated formation enthalpy for the o-MAB phase is provided. These solid solution phases, $(M'_{0.8}M''_{0.2})_5AB_2$, fulfill the stability criteria $\Delta G_{\text{solid solution}} < 0$ and $\Delta H_{o\text{-MAB}} - \Delta G_{\text{solid solution}} > 0$.

A	M'	M''	$\Delta H_{o\text{-MAB}}$ (meV/atom)	$\Delta G_{\text{solid solution}}$ (meV/atom)	Equilibrium simplex	Exp. reference
Al	Ta	Mo	6	-4	Ta_2Al, TaB, Ta_3B_2, Mo_3Al	
Al	Ta	W	-4	-6	TaB, Ta_2Al, W	
Si	Ti	Nb	42	-3	TiB, Ti_6Si_2B, Nb, Nb_5SiB_2	
Si	Ti	W	-2	-8	TiB, W, Ti_5Si_3, Ti_6Si_2B	
Si	V	Ti	81	-16	V_3B_2, V_5SiB_2, Ti_5Si_3, Ti	
Si	V	Nb	105	-13	V_5SiB_2, Nb_5SiB_2	
Si	V	Ta	88	-23	V_5SiB_2, Ta_5SiB_2	
Si	V	Cr	-16	-49	VB, V_5SiB_2, Cr_3Si	
Si	V	Mo	19	-70	VB, V_5SiB_2, Mo_3Si	
Si	V	W	8	-75	VB, W, V_5SiB_2, V_5Si_3	
Si	V	Mn	20	-10	VB, VMn_2Si, V_5SiB_2	
Si	Nb	Ti	3	-43	Nb_5SiB_2, TiB, Ti_6Si_2B, Nb	
Si	Nb	Hf	94	-12	Nb_5SiB_2, Nb_3B_2, Hf_2Si	
Si	Nb	Ta	-3	-57	Nb_5SiB_2, Ta_5SiB_2	
Si	Nb	Mo	-47	-67	NbB, Mo, Nb_5SiB_2, Nb_5Si_3	
Si	Nb	W	-32	-47	NbB, W, Nb_5SiB_2, Nb_5Si_3	
Si	Ta	Ti	15	-34	Ta_5SiB_2, Ta_3B_2, Ti_6Si_2B, Ti_5Si_3	
Si	Ta	Nb	5	-58	Ta_5SiB_2, Nb_5SiB_2	
Si	Ta	Mo	-63	-77	TaB, Ta_5SiB_2, Mo_3Si	
Si	Ta	W	-58	-66	TaB, W, Ta_5Si_3, Ta_5SiB_2	
S	Cr	Mn	49	-8	CrB, Cr_3Si, Mn_2B, MnSi	
Si	Mo	Sc	42	-24	Mo, MoB, ScB_2, $Sc_2Mo_3Si_4$	
Si	Mo	Ti	-37	-49	Mo_3Si, TiB_2, Mo	
Si	Mo	Hf	73	-2	Mo_3Si, HfB_2, Mo	
Si	Mo	Nb	21	-46	NbB, Mo_5SiB_2, Mo_3Si	
Si	Mo	Ta	7	-43	TaB, Mo_5SiB_2, Mo_3Si	
Si	Mo	W	-7	-39	MoB, W, Mo_5SiB_2, Mo_5Si_3	
Si	W	Sc	68	-27	W_2B, W_5SiB_2, Sc_5Si_3, ScB_2	
Si	W	Ti	-14	-45	W, TiB_2, WSi_2	
Si	W	V	-50	-58	W, VB, W_5SiB_2, WSi_2	
Si	W	Nb	42	-53	W_5SiB_2, W_2B, NbB, Nb_5Si_3	
Si	W	Ta	25	-48	W, TaB, W_5SiB_2, WSi_2	
Si	W	Mo	27	-33	W_2B, $MoSi_2$, Mo_5SiB_3	
Si	W	Mn	-7	-11	W_2B, MnSi	
Si	Mn	V	36	-15	Mn_2B, MnSi, VB, VMn_2Si	
Si	Mn	Cr	27	-33	Mn_2B, MnSi, CrB, Cr_3Si	
Si	Mn	Mo	118	-8	Mn_2B, MnSi, Mo_2MnB_2, MnSi	
Si	Mn	W	95	-17	Mn_2B, MnSi, W_2B	
Si	Mn	Fe	24	-25	Mn_2B, FeSi	
Si	Fe	Cr	62	-11	Fe_2B, Fe_2Si, CrB	
Si	Fe	Mn	16	-44	MnB, Fe_2B, Fe_2Si	12
Si	Fe	Co	51	-13	Fe_2B, CoSi	12, 15
Si	Co	Mn	41	-5	MnB, Fe_2B, Fe_2Si	
Si	Co	Fe	48	-12	Fe_2B, CoSi	
P	Ti	Nb	35	-14	Ti_3P, Nb_3B_2, Ti_3B_4, TiB	
P	Ti	W	-9	-11	TiB_2, Ti_3P, W	
P	V	Ti	60	-33	V_3B_2, TiVP, V_5PB_2, VB	
P	V	Nb	117	-7	V_5PB_2, Nb_5PB_2	
P	V	Ta	97	-19	V_5PB_2, Ta_5PB_2	
P	V	Cr	-30	-57	V_5PB_2, Cr_5PB_2	
P	V	Mo	26	-61	V_5PB_2, VB, Mo_3P	
P	V	W	15	-66	VB, W, V_5PB_2, $V_{12}P_7$	

P	V	Mn	-6	-31	V_5PB_2, VMnP, Mn_2B, VB	
P	Nb	Ti	-19	-54	NbB, Nb_5PB_2, Ti_3P	
P	Nb	Zr	107	-6	Nb_5PB_2, Nb_3B_2, Zr_3P, Zr_7P_4	
P	Nb	Hf	74	-29	Nb_5PB_2, NbB, Hf_3P	
P	Nb	Ta	-6	-55	Nb_5PB_2, Ta_5PB_2	
P	Nb	Mo	-42	-51	NbB, Mo, Nb_7P_4, Nb_5PB_2	
P	Nb	W	-18	-19	NbB, W, Nb_7P_4, Nb_5PB_2	
P	Ta	Ti	3	-36	Ta_3B_2, Ta_5PB_2, Ti_2P	
P	Ta	Nb	7	-55	Ta_5PB_2, Nb_5PB_2	
P	Ta	Mo	-47	-51	TaB, Ta_5PB_2, Mo_3P	
P	Cr	V	10	-56	Cr_5PB_2, V_5PB_2	
P	Cr	Mo	104	-18	Cr_5PB_2, Mo_2CrB_2, MoP, Mo_3P	
P	Cr	W	88	-21	Cr_5PB_2, W_2B, CrP	
P	Cr	Mn	1	-45	Cr_5PB_2, Mn_5PB_2	
P	Cr	Fe	32	-10	CrFeP, CrB, Cr_5B_3	
P	Cr	Co	33	-10	Co_2P, Cr_5PB_2, CrB, Cr_5B_3	
P	Mo	Ti	-51	-69	Mo_3P, TiB_2, Mo	
P	Mo	Nb	34	-42	MoB, Mo, NbP	
P	Mo	Ta	21	-39	TaB, Mo_3P, MoB	
P	Mo	W	25	-14	MoB, W, MoP, Mo_3P	
P	W	Ti	37	-5	W_2B, TiP	
P	W	V	-6	-19	W_2B, VP	
P	Mn	V	37	-35	Mn_25PB_2, Mn_2B, VMnP, VB	
P	Mn	Cr	21	-48	Mn_5PB_2, Cr_5PB_2	
P	Mn	Mo	128	-9	Mn_5PB_2, Mn_2P, Mo_2MnB_2	
P	Mn	W	115	-14	Mn_5PB_2, W_2B, MnP	
P	Mn	Fe	13	-27	MnFeP, Mn_2B, MnB	
P	Mn	Co	28	-19	Mn_5PB_2, Mn_2B, MnB, Co_2P	
P	Fe	Cr	63	-22	Fe_5PB_2, Fe_2B, CrFeP, CrB	
P	Fe	Mn	18	-42	MnFeP, Fe_2B, FeB	[12]
P	Fe	Co	36	-12	CoFeP, Fe_2B, FeB	[21]
P	Co	Mn	66	-2	CoB, Co_2P, Mn_2B, Co	
P	Co	Fe	73	-2	CoB, Co_2P, CoFe, CoFeP	[21]
Ga	V	Cr	21	-5	V_3B_2, Cr, V_6Ga_5, V_2Ga_5	
Ga	V	Mo	59	-13	V_3B_2, Mo_3Ga, V_3Ga, V_6Ga_5	
Ga	V	W	52	-14	V_3B_2, W, V_6Ga_5, V_2Ga_5	
Ga	Nb	Ti	45	-16	Nb_3B_2, Ti_2Ga, Nb_5Ga_3, Ta	
Ga	Nb	Ta	22	-30	Nb_3B_2, Nb_5Ga_3, Ta_3B_2, Nb	
Ga	Nb	Mo	-18	-27	NbB, Mo, Nb_3B_2, Nb_5Ga_3	
Ga	Nb	W	-2	-6	NbB, W, Nb_3B_2, Nb_5Ga_3	
Ga	Ta	Ti	64	0	Ta_3B_2, Ti_2Ga, Ta_5Ga_3, Ta	
Ga	Ta	Nb	31	-27	Ta_3B_2, Ta, Nb_5Ga_3, Ta_5Ga_3	
Ga	Ta	Mo	-39	-42	Ta_3B_2, Mo_3Ga, TaB, Ta_5Ga_3	
Ga	Mo	Nb	67	-1	MoB, Mo_3Ga, NbB	
Ga	Mo	W	34	-2	MoB, W, Mo_3Ga, $MoGa_4$	
Ga	W	Ta	70	-4	W, W_2B, TaB, Ga	
Ge	Ti	Nb	30	-7	TiB, Nb, Ti_5Ge_3, Ti	
Ge	V	Nb	100	-13	V_5Ge_3, Nb_5Ge_3, V_3Ge, V_5GeB_2	
Ge	V	Ta	82	-25	V_5GeB_2, Ta_5GeB_2	
Ge	V	Cr	-15	-49	VB, V_4GeB_2, Cr_3Ge	
Ge	V	Mo	23	-62	VB, V_4GeB_2, Mo_3Ge	
Ge	V	W	24	-52	VB, W, V_5Ge_3, V_5SiB_2	
Ge	V	Mn	19	-17	VB, VMn, VMn_2Ge, V_5Ge_3	
Ge	V	Fe	28	-7	VB, Fe, V_5Ge_3, V_5SiB_2	
Ge	Nb	Ti	16	-37	Nb_3B_2, Nb_5GeB_2, Ti_5Ge_3, Nb	
Ge	Nb	Hf	103	-8	Hf_2Ge, Nb_3B_2, Nb_5GeB_2	
Ge	Nb	Ta	-4	-57	Nb_5GeB_2, Ta_5GeB_2	
Ge	Nb	Mo	-46	-64	NbB, Mo, Nb_5Ge_3, Nb_5GeB_2	
Ge	Nb	W	-28	-38	NbB, W, Nb_5Ge_3, Nb_5GeB_2	
Ge	Ta	Ti	46	-12	Ta_3B_2, Ta_5GeB_2, Ti_5Ge_3, Ta	

Ge	Ta	Nb	6	-57	Ta_5GeB_2, Nb_5GeB_2
Ge	Ta	Mo	-55	-69	TaB, Ta_5GeB_2, Mo_3Ge
Ge	Ta	W	-48	-53	TaB, W, Ta_5Ge_3, Ta_5GeB_2
Ge	Mo	Ti	-14	-35	Mo_3Ge, TiB_2, Mo
Ge	Mo	V	-17	-19	VB, Mo_3Ge, MoB
Ge	Mo	Nb	36	-31	NbB, Mo_3Ge, MoB
Ge	Mo	Ta	26	-23	TaB, Mo_3Ge, MoB
Ge	Mo	W	20	-9	MoB, W, Mo_3Ge, $MoGe_2$
Ge	Mn	Cr	47	-10	Mn_2B, CrB, Mn_3Ge, $MnGe$
Ge	Mn	Fe	16	-29	Mn_2B, $MnGe$, Fe_2B
Ge	Fe	Cr	53	-18	Fe_2B, $FeGe$, Cr_5B_3, Cr_3Ge
Ge	Fe	Mn	19	-40	Fe_2B, $FeGe$, Mn_2B
Ge	Co	Mn	27	-9	Co, CoB, $CoGe$, Mn_2B
Ge	Co	Fe	39	-13	CoB, Co, $CoGe$, Fe_2B

Table S7. Calculated structural information for predicted stable *o*-MAB phases, $M'_4M''A$B$_2$, listed in Table S5.

A	M′	M″	a (Å)	c (Å)	Wyckoff sites
Si	Ti	Mo	6.09359	11.43590	Ti 16l (0.67618, 0.67618, 0.13157) Mo 4c (0.00000, 0.00000, 0.00000) Si 4a (0.00000, 0.00000, 0.25000) B 8h (0.89246, 0.89246, 0.00000)
Si	Ti	Mn	5.87927	11.58850	Ti 16l (0.67656, 0.67656, 0.13068) Mn 4c (0.00000, 0.00000, 0.00000) Si 4a (0.00000, 0.00000, 0.25000) B 8h (0.88731, 0.88731, 0.00000)
Si	Nb	V	6.14802	11.63100	Nb 16l (0.67077, 0.67077, 0.13583) V 4c (0.00000, 0.00000, 0.00000) Si 4a (0.00000, 0.00000, 0.25000) B 8h (0.88186, 0.88186, 0.00000)
Si	Nb	Cr	6.10266	11.59550	Nb 16l (0.67063, 0.67063, 0.13614) Cr 4c (0.00000, 0.00000, 0.00000) Si 4a (0.00000, 0.00000, 0.25000) B 8h (0.88061, 0.88061, 0.00000)
Si	Ta	V	6.11481	11.52270	Ta 16l (0.66941, 0.66941, 0.13660) V 4c (0.00000, 0.00000, 0.00000) Si 4a (0.00000, 0.00000, 0.25000) B 8h (0.87875, 0.87875, 0.00000)
Si	Ta	Cr	6.06663	11.50100	Ta 16l (0.66928, 0.66928, 0.13702) Cr 4c (0.00000, 0.00000, 0.00000) Si 4a (0.00000, 0.00000, 0.25000) B 8h (0.87818, 0.87818, 0.00000)
Si	Ta	Mn	6.04995	11.51720	Ta 16l (0.66910, 0.66910, 0.13737) Mn 4c (0.00000, 0.00000, 0.00000) Si 4a (0.00000, 0.00000, 0.25000) B 8h (0.87903, 0.87903, 0.00000)
Si	Mo	V	5.97560	11.10880	Mo 16l (0.66767, 0.66767, 0.13688) V 4c (0.00000, 0.00000, 0.00000) Si 4a (0.00000, 0.00000, 0.25000) B 8h (0.87877, 0.87877, 0.00000)
Si	Mo	Cr	5.93417	11.09640	Mo 16l (0.66769, 0.66769, 0.13677) Cr 4c (0.00000, 0.00000, 0.00000) Si 4a (0.00000, 0.00000, 0.25000) B 8h (0.87685, 0.87685, 0.00000)
Si	Mo	Mn	5.93248	11.13690	Mo 16l (0.66896, 0.66896, 0.13607) Mn 4c (0.00000, 0.00000, 0.00000) Si 4a (0.00000, 0.00000, 0.25000) B 8h (0.87918, 0.87918, 0.00000)
Si	W	Cr	5.95633	10.96220	W 16l (0.66464, 0.66464, 0.13832) Cr 4c (0.00000, 0.00000, 0.00000) Si 4a (0.00000, 0.00000, 0.25000) B 8h (0.87163, 0.87163, 0.00000)
P	Ti	Cr	5.89048	11.32240	Ti 16l (0.67620, 0.67620, 0.13318) Cr 4c (0.00000, 0.00000, 0.00000) P 4a (0.00000, 0.00000, 0.25000) B 8h (0.88762, 0.88762, 0.00000)
P	Ti	Mo	6.02784	11.31580	Ti 16l (0.67516, 0.67516, 0.13451) Mo 4c (0.00000, 0.00000, 0.00000) P 4a (0.00000, 0.00000, 0.25000) B 8h (0.89106, 0.89106, 0.00000)
P	Ti	Mn	5.83625	11.34670	Ti 16l (0.67492, 0.67492, 0.13430) Mn 4c (0.00000, 0.00000, 0.00000) P 4a (0.00000, 0.00000, 0.25000) B 8h (0.88600, 0.88600, 0.00000)
P	Nb	V	6.10357	11.52040	Nb 16l (0.67047, 0.67047, 0.13798) V 4c (0.00000, 0.00000, 0.00000) P 4a (0.00000, 0.00000, 0.25000) B 8h (0.88263, 0.88263, 0.00000)

P	Nb	Cr	6.05282	11.53200	Nb 16l (0.67073, 0.67073, 0.13782) Cr 4c (0.00000, 0.00000, 0.00000) P 4a (0.00000, 0.00000, 0.25000) B 8h (0.88094, 0.88094, 0.00000)
P	Nb	Mn	6.02485	11.67340	Nb 16l (0.67221, 0.67221, 0.13746) Mn 4c (0.00000, 0.00000, 0.00000) P 4a (0.00000, 0.00000, 0.25000) B 8h (0.88413, 0.88413, 0.00000)
P	Ta	V	6.06752	11.43000	Ta 16l (0.66905, 0.66905, 0.13861) V 4c (0.00000, 0.00000, 0.00000) P 4a (0.00000, 0.00000, 0.25000) B 8h (0.87958, 0.87958, 0.00000)
P	Ta	Cr	6.01376	11.44970	Ta 16l (0.66940, 0.66940, 0.13869) Cr 4c (0.00000, 0.00000, 0.00000) P 4a (0.00000, 0.00000, 0.25000) B 8h (0.87850, 0.87850, 0.00000)
P	Ta	W	6.12238	11.50550	Ta 16l (0.66709, 0.66709, 0.14079) W 4c (0.00000, 0.00000, 0.00000) P 4a (0.00000, 0.00000, 0.25000) B 8h (0.87986, 0.87986, 0.00000)
P	Ta	Mn	5.97930	11.58650	Ta 16l (0.67079, 0.67079, 0.13824) Mn 4c (0.00000, 0.00000, 0.00000) P 4a (0.00000, 0.00000, 0.25000) B 8h (0.88153, 0.88153, 0.00000)
P	Mo	V	5.91680	11.14370	Mo 16l (0.66999, 0.66999, 0.13735) V 4c (0.00000, 0.00000, 0.00000) P 4a (0.00000, 0.00000, 0.25000) B 8h (0.88160, 0.88160, 0.00000)
P	Mo	Cr	5.85706	11.23330	Mo 16l (0.67062, 0.67062, 0.13711) Cr 4c (0.00000, 0.00000, 0.00000) P 4a (0.00000, 0.00000, 0.25000) B 8h (0.88011, 0.88011, 0.00000)
P	Mo	Mn	5.83579	11.31380	Mo 16l (0.67203, 0.67203, 0.13680) Mn 4c (0.00000, 0.00000, 0.00000) P 4a (0.00000, 0.00000, 0.25000) B 8h (0.88256, 0.88256, 0.00000)
Ga	Ti	Mo	6.10604	11.72840	Ti 16l (0.67615, 0.67615, 0.12810) Mo 4c (0.00000, 0.00000, 0.00000) Ga 4a (0.00000, 0.00000, 0.25000) B 8h (0.89273, 0.89273, 0.00000)
Ga	Ta	V	6.15337	11.66420	Ta 16l (0.66929, 0.66929, 0.13310) V 4c (0.00000, 0.00000, 0.00000) Ga 4a (0.00000, 0.00000, 0.25000) B 8h (0.87611, 0.87611, 0.00000)
Ga	Ta	Cr	6.09898	11.64560	Ta 16l (0.66890, 0.66890, 0.13403) Cr 4c (0.00000, 0.00000, 0.00000) Ga 4a (0.00000, 0.00000, 0.25000) B 8h (0.87573, 0.87573, 0.00000)
Ga	Ta	W	6.21049	11.67240	Ta 16l (0.66664, 0.66664, 0.13604) W 4c (0.00000, 0.00000, 0.00000) Ga 4a (0.00000, 0.00000, 0.25000) B 8h (0.87756, 0.87756, 0.00000)
Ge	Ti	Mo	6.10582	11.59260	Ti 16l (0.67572, 0.67572, 0.12941) Mo 4c (0.00000, 0.00000, 0.00000) Ge 4a (0.00000, 0.00000, 0.25000) B 8h (0.89202, 0.89202, 0.00000)
Ge	Ti	W	6.09311	11.64180	Ti 16l (0.67529, 0.67529, 0.12969) W 4c (0.00000, 0.00000, 0.00000) Ge 4a (0.00000, 0.00000, 0.25000) B 8h (0.89053, 0.89053, 0.00000)
Ge	Ti	Mn	5.88630	11.78260	Ti 16l (0.67613, 0.67613, 0.12828) Mn 4c (0.00000, 0.00000, 0.00000) Ge 4a (0.00000, 0.00000, 0.25000) B 8h (0.88677, 0.88677, 0.00000)

Ge	Nb	V	6.18025	11.71940	Nb 16l (0.66948, 0.66948, 0.13393) V 4c (0.00000, 0.00000, 0.00000) Ge 4a (0.00000, 0.00000, 0.25000) B 8h (0.87990, 0.87990, 0.00000)
Ge	Nb	Cr	6.13063	11.70240	Nb 16l (0.66883, 0.66883, 0.13432) Cr 4c (0.00000, 0.00000, 0.00000) Ge 4a (0.00000, 0.00000, 0.25000) B 8h (0.87778, 0.87778, 0.00000)
Ge	Ta	V	6.14965	11.59720	Ta 16l (0.66786, 0.66786, 0.13468) V 4c (0.00000, 0.00000, 0.00000) Ge 4a (0.00000, 0.00000, 0.25000) B 8h (0.87637, 0.87637, 0.00000)
Ge	Ta	Cr	6.09706	11.59320	Ta 16l (0.66731, 0.66731, 0.13520) Cr 4c (0.00000, 0.00000, 0.00000) Ge 4a (0.00000, 0.00000, 0.25000) B 8h (0.87508, 0.87508, 0.00000)
Ge	Ta	Mn	6.08346	11.61750	Ta 16l (0.66741, 0.66741, 0.13544) Mn 4c (0.00000, 0.00000, 0.00000) Ge 4a (0.00000, 0.00000, 0.25000) B 8h (0.87690, 0.87690, 0.00000)

Table S8. Atomic radius and electronegativity considered for M and A.[24, 25]

| M	Atomic radius r_M (Å)	Electronegativity ρ_M (Pauling scale)	A	Atomic radius r_A (Å)	Electronegativity ρ_A (Pauling scale)
Sc	1.62	1.36	Al	1.43	1.61
Y	1.80	1.22	Si	1.38	1.90
Ti	1.47	1.54	P	1.15	2.19
Zr	1.60	1.33	Ga	1.40	1.81
Hf	1.59	1.30	Ge	1.44	2.01
V	1.35	1.63			
Nb	1.46	1.60			
Ta	1.46	1.50			
Cr	1.29	1.66			
Mo	1.39	2.16			
W	1.39	2.36			
Mn	1.27	1.55			
Fe	1.26	1.83			
Co	1.25	1.88			
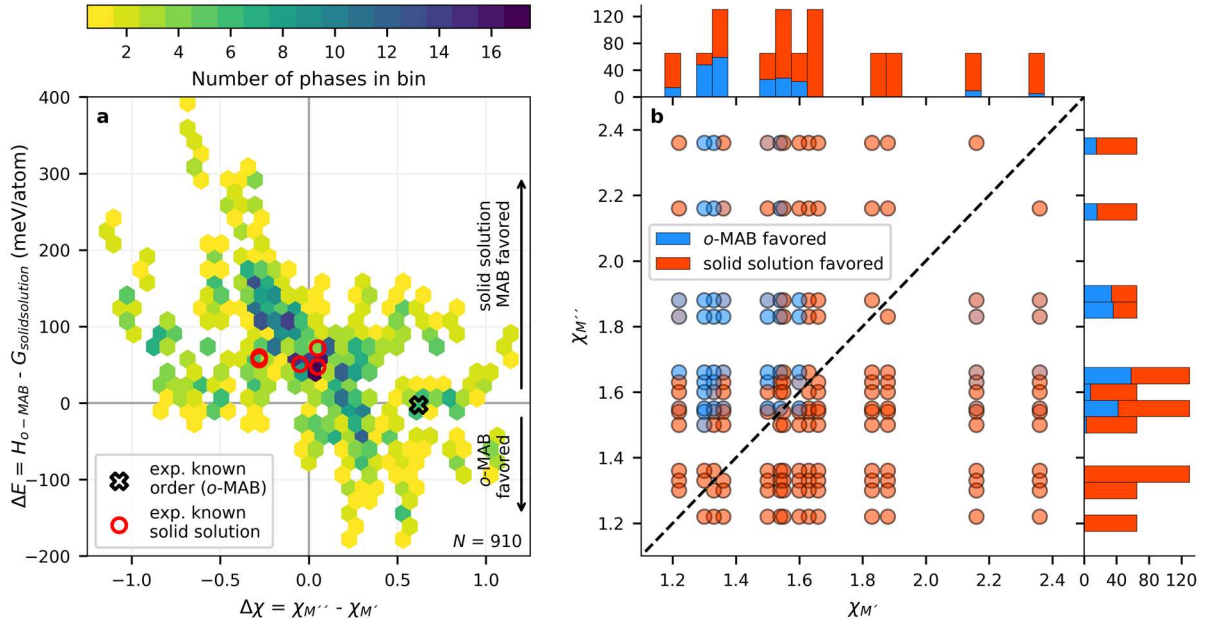
Figure S6. (a) Hexbin plot showing the energy difference of chemical order ($\Delta H_{o\text{-MAB}}$) and chemical disorder ($\Delta G_{\text{solid solution}}$ at 2000 K) as function of electronegativity difference, $\Delta\chi$, of M'' and M' for all 910 compositions. The color of a hexabin represent the number of stable phases. Experimentally known o-MAB phase is indicated by a black cross and solid solution MAB phases by red circles. (b) Electronegativity χ of M'' as function of M' for stable composition where the color of each data point represents if order (blue) or solid solution is lowest in energy for a given composition. Histograms are given for each axis with a bin size of 0.05.
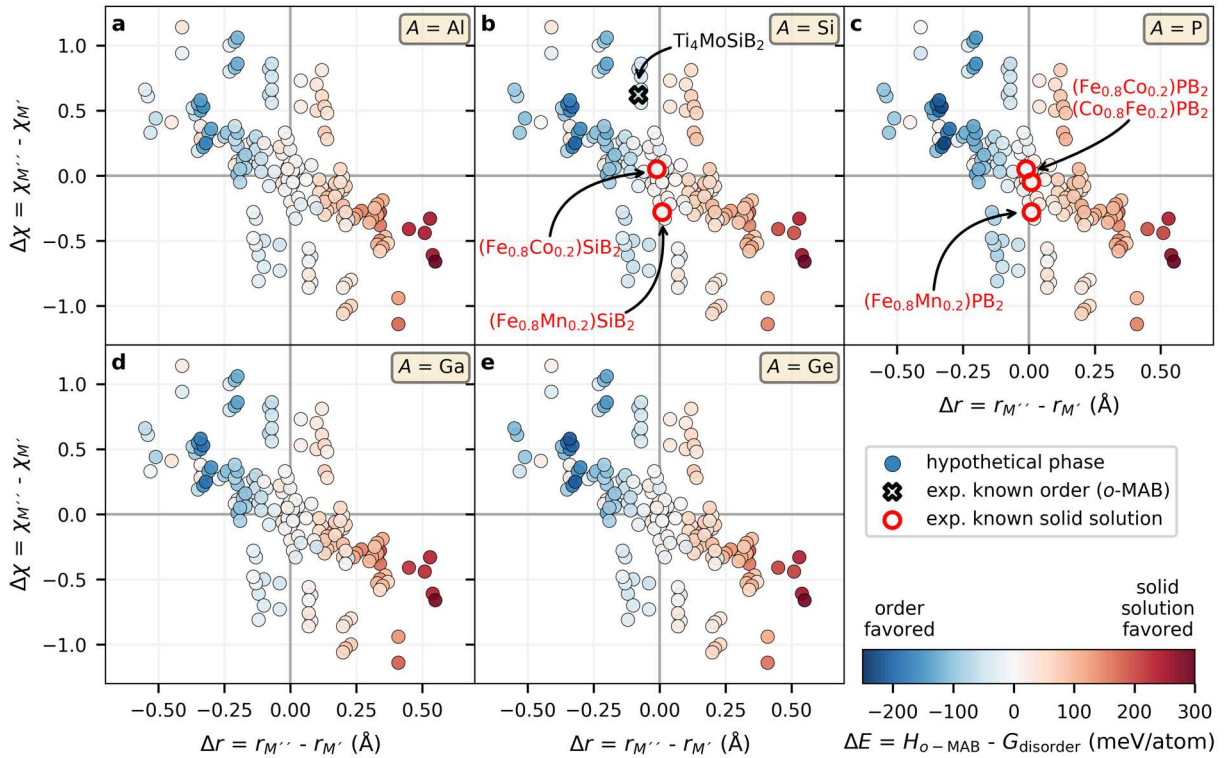

Figure S7. Electronegativity difference of M'' and M' as function of size difference of M' and M'' for A being (a) Al, (b) Si, (c) P, (d) Ga and (e) Ge. The color of each data point represents the energy difference ΔE between chemically ordered $M'_4 M'' A B_2$ and solid solution $(M'_{0.8} M''_{0.2})_5 A B_2$ where blue color indicate favor for ordered o-MAB and red favor solid solution $(M'_{0.8} M''_{0.2})_5 A B_2$.
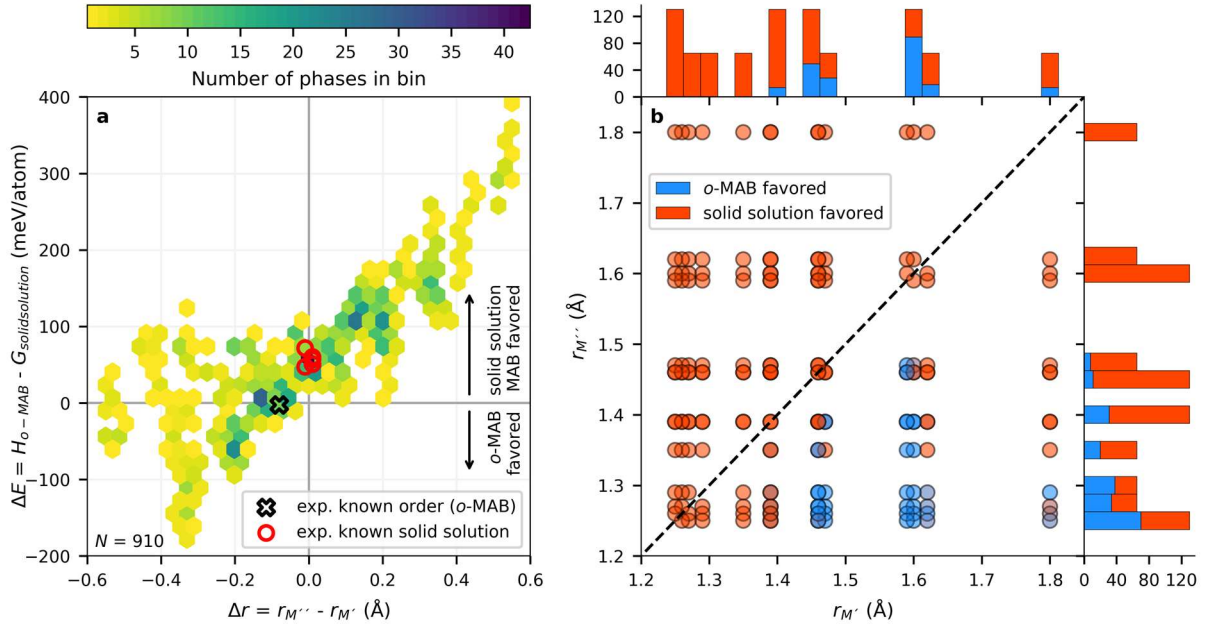
Figure S8. (a) Hexbin plot showing the energy difference of chemical order ($\Delta H_{o\text{-MAB}}$) and chemical disorder ($\Delta G_{\text{solid solution}}$ at 2000 K) as function of size difference, Δr, of M'' and M' for all 910 compositions. The color of a hexabin represent the number of stable phases. The experimentally known o-MAB phase is indicated by a black cross and solid solution MAB phases by red circles. (b) Atomic size r of M'' as function of M' for stable composition where the color of each data point represents if order (blue) or solid solution is lowest in energy for a given composition. Histograms are given for each axis with a bin size of 0.025 Å.
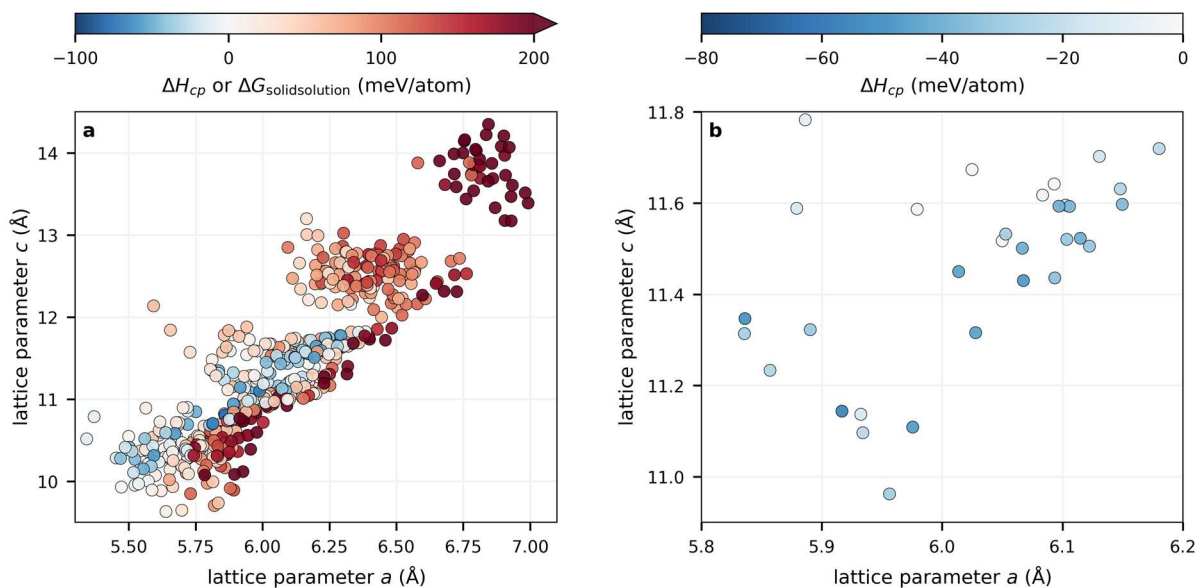
Figure S9. Calculated lattice parameters a and c for (a) all 910 compositions and (b) the 36 predicted stable o-MAB phases. Coloring of each data point refers to the calculated formation enthalpy or free Gibbs free energy of formation where blue indicate stable and red not stable.
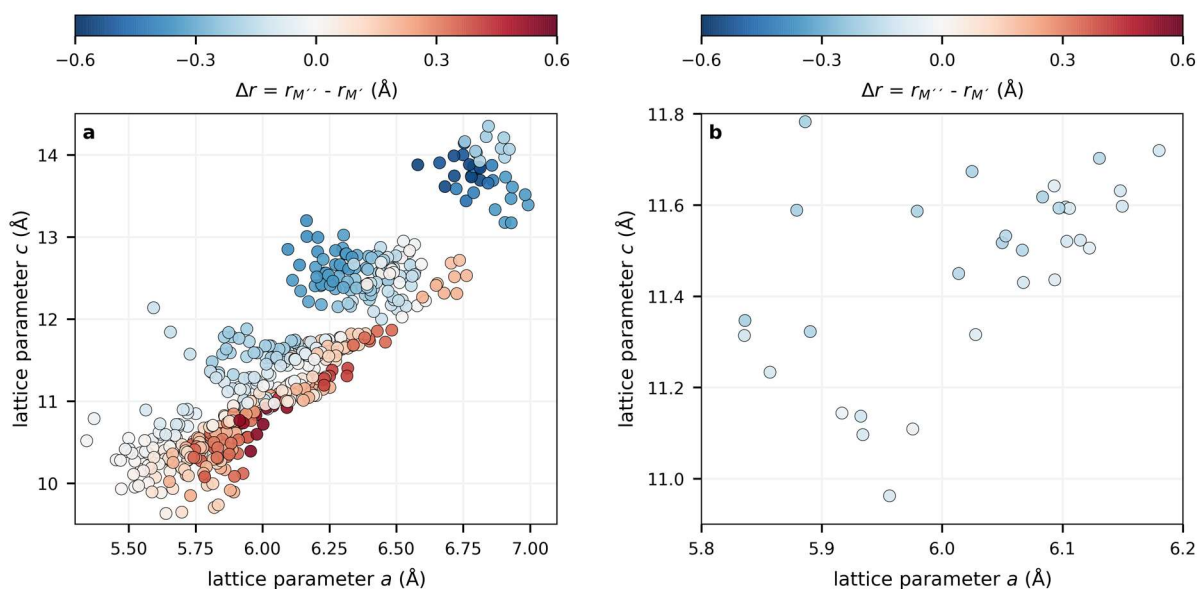

Figure S10. Calculated lattice parameters a and c for (a) all 910 compositions and (b) the 36 predicted stable o-MAB phases. Coloring of each data point refers to the size difference, Δr, of M'' and M' where blue indicate $r_{M''} < r_{M'}$ and red $r_{M''} > r_{M'}$.

SUPPLEMENTARY REFERENCES

(1)   Nunes, C. A.; de Lima, B. B.; Coelho, G. C.; Suzuki, P. A., Isothermal Section of the V-Si-B System at 1600 °C in the V-VSi$_2$-VB Region. *J. Phase Equilib. Diff.* **2009,** *30*, 345-350.

(2)   Rodrigues, G.; Nunes, C. A.; Suzuki, P. A.; Coelho, G. C., Lattice parameters and thermal expansion of the T$_2$-phase of the Nb–Si–B system investigated by high-temperature X-ray diffraction. *Intermetallics* **2004,** *12*, 181-188.

(3)   Brauner, A.; Nunes, C. A.; Bortolozo, A. D.; Rodrigues, G.; Machado, A. J. S., Superconductivity in the new Nb$_5$Si$_{3-x}$B$_x$ phase. *Solid State Commun.* **2009,** *149*, 467-470.

(4)   Kudielka, H.; Nowotny, H.; Findeisen, G., Untersuchungen in den Systemen: V–B, Nb–B, V−B−Si und Ta−B−Si. *Monatsh. Chem.* **1957,** *88*, 1048-1055.

(5)   Nowotny, H.; Lux, B.; Kudielka, H., Das Verhalten metallreicher, hochschmelzender Silizide gegenüber Bor, Kohlenstoff, Stickstoff und Sauerstoff. *Monatsh. Chem.* **1956,** *87*, 447-470.

(6)   Silvestroni, L.; Sciti, D., Densification of ZrB2–TaSi2 and HfB2–TaSi2 Ultra-High-Temperature Ceramic Composites. *J. Am. Ceram. Soc.* **2011,** *94*, 1920-1930.

(7)   Nowotny, H.; Dimakopoulou, E.; Kudielka, H., Untersuchungen in den Dreistoffsystemen: Molybdän-Silizium-Bor, Wolfram-Silizium-Bor und in dem System: VSi$_2$-TaSi$_2$. *Monatsh. Chem.* **1957,** *88*, 180-192.

(8)   MacHado, A. J. S.; Costa, A. M. S.; Nunes, C. A.; Dos Santos, C. A. M.; Grant, T.; Fisk, Z., Superconductivity in Mo$_5$SiB$_2$. *Solid State Commun.* **2011,** *151*, 1455-1458.

(9)   Fukuma, M.; Kawashima, K.; Maruyama, M.; Akimitsu, J., Superconductivity in W$_5$SiB$_2$ with the T2 Phase Structure. *Journal of the Physical Society of Japan* **2011,** *80*, 024702.

(10)   de Almeida, D. M.; Bormio-Nunes, C.; Nunes, C. A.; Coelho, A. A.; Coelho, G. C., Magnetic characterization of Mn$_5$SiB$_2$ and Mn$_5$Si$_3$ phases. *J. Magn. Magn. Mater.* **2009,** *321*, 2578-2581.

(11)   Aronsson, B.; Engström, I., X-Ray Investigations on M-Si-B Systems (M = Mn, Fe, Co). II. Some Features of the Fe-Si-B and Mn-Si-B Systems. *Acta Chem Scand A* **1960,** *14*, 1403-1413.

(12)   McGuire, M. A.; Parker, D. S., Magnetic and structural properties of ferromagnetic Fe$_5$PB$_2$ and Fe$_5$SiB$_2$ and effects of Co and Mn substitutions. *J. Appl. Phys.* **2015,** *118*, 163903.

(13)   Werwiński, M.; Kontos, S.; Gunnarsson, K.; Svedlindh, P.; Cedervall, J.; Höglin, V.; Sahlberg, M.; Edström, A.; Eriksson, O.; Rusz, J., Magnetic properties of Fe$_5$SiB$_2$ and its alloys with P, S, and Co. *Phys. Rev. B* **2016,** *93*, 174412.

(14)   Hedlund, D.; Cedervall, J.; Edström, A.; Werwiński, M.; Kontos, S.; Eriksson, O.; Rusz, J.; Svedlindh, P.; Sahlberg, M.; Gunnarsson, K., Magnetic properties of the Fe$_5$SiB$_2$-Fe$_5$PB$_2$ system. *Phys. Rev. B* **2017,** *96*, 094433.

(15)   Hirian, R.; Isnard, O.; Pop, V.; Benea, D., Investigations on the magnetic properties of the Fe$_{5-x}$Co$_x$SiB$_2$ alloys by experimental and band structure calculation methods. *J. Magn. Magn. Mater.* **2020,** *505*, 166748.

(16)   Corrêa, L. E.; da Luz, M. S.; de Lima, B. S.; Cigarroa, O. V.; da Silva, A. A. A. P.; Coelho, G. C.; Fisk, Z.; Machado, A. J. S., Ta$_5$GeB$_2$: New T2 superconductor phase. *J. Alloys Compd.* **2016,** *660*, 44-47.

(17)   Baurecht, H. E.; Boller, H.; Nowotny, H., Röntgenographische Untersuchunge in den Dreistoffen Cr−P−C, Cr−As−C und Cr−P−B. *Monatsh. Chem.* **1971,** *102*, 373-384.

(18)   McGuire, M. A.; Parker, D. S., Superconductivity at 9 K in Mo$_5$PB$_2$ with evidence for multiple gaps. *Phys. Rev. B* **2016,** *93*, 064507.

(19)   Il'nitskaya, O. N.; Kuz'ma, Y. B., Diagram of phase equilibria in the MO-P-B system in the range 0–0.67 at. fraction of P. *Soviet Powder Metallurgy and Metal Ceramics* **1985,** *24*, 226-228.

(20)   Rundqvist, S., X-ray investigations of the ternary system Fe-P-B. Some features of the systems Cr-P-B, Mn-P-B, Co-PB and Ni-P-B. *Acta Chem. Scand* **1962,** *16*, 1-19.

(21)   Cedervall, J.; Nonnet, E.; Hedlund, D.; Häggström, L.; Ericsson, T.; Werwiński, M.; Edström, A.; Rusz, J.; Svedlindh, P.; Gunnarsson, K.; Sahlberg, M., Influence of Cobalt Substitution on the Magnetic Properties of Fe$_5$PB$_2$. *Inorg. Chem.* **2018,** *57*, 777-784.

(22)   Fukuma, M.; Kawashima, K.; Akimitsu, J. In *Substitution effect on the superconductivity in W$_{5-x}$Ta$_x$SiB$_2$ with the T2 phase structure*, Journal of Physics: Conference Series, 2012.

(23)   Dahlqvist, M.; Zhou, J.; Persson, I.; Ahmed, B.; Lu, J.; Halim, J.; Tao, Q.; Palisaitis, J.; Thörnberg, J.; Helmer, P.; Hultman, L.; Persson, P. O. Å.; Rosen, J., Out-Of-Plane Ordered Laminate Borides and Their 2D Ti-Based Derivative from Chemical Exfoliation. *Adv. Mater.* **2020,** *accepted for publication*.

(24)   Greenwood, N. N.; Earnshaw, A., *Chemistry of the Elements*. 2nd ed.; Butterworth-Heinemann: 1997.

(25)   Huheey, J. E.; Keiter, E. A.; Keiter, R. L., *Inorganic Chemistry : Principles of Structure and Reactivity*. 4th ed.; HarperCollins: New York, USA, 1993.